A SMART MICROFLUIDIC SYSTEM INTEGRATED WITH PRESSURE SENSORS AND FLOW SENSOR BASED ON ELECTROCHEMICAL IMPEDANCE METHODS

Longjun Tang, Jingquan Liu, Wen Hong, Tao Wang, Xiaolin Wang, Xiang Chen, Bin Yang, and Chunsheng Yang

National Key Laboratory of Science and Technology on Micro/Nano Fabrication, Department of Micro/Nano-electronics, Shanghai Jiao Tong University, Shanghai, P.R. China

Collaborative Innovation Center of IFSA, Shanghai Jiao Tong University, Shanghai, P.R. China

ABSTRACT

We report on a smart microfluidic system with multiple micro sensors integrated in the channel. It consists of a standard PDMS channel, and a smart substrate which has six bubble pressure sensors and a flow sensor all based on electrochemical impedance methods. This system will allow, for the first time, directly and simultaneously monitoring of multiple parameters in the channel of microfluidic systems, including the monitoring of local pressures, flow rate, particles, cells, and so on.

INTRODUCTION

Flow monitoring and control are fundamental requirements for microfluidic or lab-on-a-chip systems [1-10]. However, flow and pressure measurements of modern microfluidic systems are still fully rely on external measuring equipments, which result in narrow bandwidth, complex piping systems, and high cost. There are two major reasons for this low integration of modern microfluidic systems. One obvious limitation is that most commercial sensors are macroscale in their dimensions, which are too large to be accommodated in microchannels. Although MEMS pressure sensors have got great progress in the past decades, few of them are specially designed for fluids at the microscale. The footprints of the state-of-art pressure sensors are still at the millimeter scale after packaging [11-12]. The other reason is that commercially available sensors does not match the disposable nature of streamline lab-on-a-chip devices. The commercial sensors always have front-end temperature compensation and signal amplification, which are oriented towards long-term and wide-range applications. But a typical microfluidic chip may only work several minutes to several hours at one time. This mismatch, and the large size of commercial sensors, along with the overcapacity of general sensors and the resulting high cost, hinder the development of the integration of multiple sensors into microfluidic systems. Therefore, specific sensing mechanics and processing technologies towards microfluidic environment are essential to realize the next generation of microfluidic system with high integration and high intelligence.

Many groups have tried different ways to fabricate pressure sensing elements compatible with microfluidic chips and integrate them into microchannels [3-10]. However, all of them are still too large, from millimeters to centimeters, and need redesign of the channel. Moreover, to our knowledge, there is no existing way can fabricate multiple sensors within a standard PDMS microfluidic chip. Because the fabrication process of pressure sensors are always not compatible with other sensors, such as flow sensor, thus making integration of multiple sensors to microchannels really challenging.

This paper aims to develop a new design of microfluidic system which is able to monitor multiple fluidic parameters within the channel simultaneously, in real time, and also with electrical readouts. For principle demonstration, we developed two types of sensors, pressure sensor and flow sensor, and seamlessly integrated them into standard PDMS channels for local pressure and flow condition monitoring.

CONCEPT AND DESIGN

As shown in Fig. 1, the smart microfluidic system consists of a smart substrate and a standard PDMS channel. The sensors are fabricated on the substrate. The PDMS channel is fabricated through a separated process. Then the two parts are aligned and bonded together. As a results, the sensors are localized within the channel at their desired locations. Here, we have two types of sensor, the pressure sensor (PS) and the flow sensor (FS). These two types of sensors are both based on electrochemical impedance (EI) methods, and also process-compatible, which means they can be fabricated through the same series of micromachining processes on one chip.

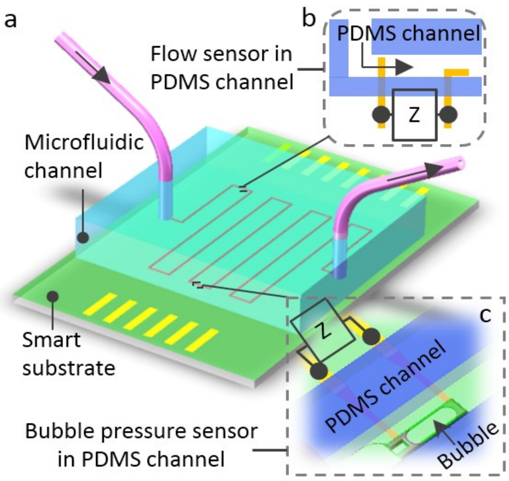

Fig. 1: Schematic view of the smart microfluidic system. (a) The system consists of two subsystems, the smart substrate integrated with sensors, and the microfluidic channel based on standard soft lithography. (b) The flow sensor (FS) has two electrodes in the channel to sense the flow condition. (c) The bubble pressure sensor (PS) utilizes a confined microbubble to sense pressure and pressure changes within the channel.

The FS consists of two electrodes within the channel (Fig. 1 b). The impedance between the two electrodes can reflect the flow condition between them [13-14]. A bubble spontaneously formed and confined in a micro chamber of the bubble PS is employed as the sensing element for measuring fluid pressures (Fig. 1 c) [15]. The length of the bubble, which is indirectly characterized by measuring the impedance across two electrodes located at each side of the bubble, can reflect the fluid pressure.

FABRICATION

Fabrication of the smart substrate

Surface micromachining techniques performed at low temperature (<100 ºC) are utilized for the fabrication of the smart substrate (Fig. 2). The smart substrate consists of two Parylene-C layers and a metal layer. Before the deposition of the first Parylene layer (5 µm), the glass substrate was treated with A-174 to enhance the adhesion between Parylene and glass. The electrodes of the bubble PS and the FS were patterned through a lift-off process or chemical etching of the deposited Au/ Cr layer (Au, 300 nm, Cr, 15 nm). Then a sacrificial photoresist (PR), which was used to define the micro chamber of the bubble PS, was spin coated to a thickness of 15 µm. Here, the sidewall angle of the sacrificial PR is smaller than 30°, as we have found that for a steady and reliable generation of micro bubbles in the micro chamber, sharp corners in the bottom of the micro chamber are necessary. This feature of PR was achieved by placing a PVC film (thickness of 180-200 µm) between the mask and the sacrificial PR (AZ 4620) when conducting the exposure (Karl Suss MA6, h line, 9 mW/ cm^2, 130 s). A subsequent baking (90 ºC for 5 min) was performed to smooth the edge of the sacrificial PR. The second Parylene layer (4 µm) was deposited on the sacrificial photoresist to form the micro chamber. After a subsequent RIE process, the sacrificial PR was dissolved in acetone. A half-sealed micro chamber of the bubble PS was completely developed.

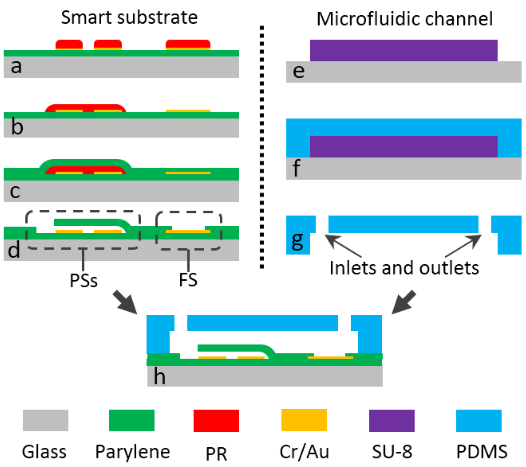

Fig. 2: Process of the device microfabrication. (a) Robustly adhere Parylene layer to glass wafer, and pattern the electrodes (b) Sacrificial PR of the bubble PS. (c) The final Encapsulation layer of the sensors. (d) Etch and release the sacrificial PR. (e-g) Standard soft lithography for the PDMS channel. (g) Bond the PDMS channel to the smart substrate using a chemical gluing strategy.

As shown in Fig. 2, the difference between the PS and the bubble PS is that, the FS does not have the sacrificial PR and the micro chamber.

Bonding of PDMS with Parylene-C

The PDMS channel (200×100×160 µm^3, width ×height ×length) was fabricated through a standard soft lithography. The mold was made by SU-8 on glass wafer. PMDS was mixed (ratio of 1:10), degassed, and poured onto the SU-8 mold, then cured (60 ºC, 2 h). The PDMS channel was peeled off, diced into chips, and punched to form the inlet and outlet. In order to facilely bond PDMS to Parylene-C at low pressures and room temperature, and also provide sufficient time for their alignment. The Parylene-C-based smart substrate was activated with oxygen plasma, and subsequently treated with 1% 3-Aminopropyltriethoxysilane (APTES, 99%) solution. The PDMS channel was also activated with oxygen plasma, and treated with 1% 3-glycidoxypropyltrimethoxysilane (GPTMS, 98%) solution. The smart substrate and the PDMS chip were then air dried, aligned to ensure the sensors were in the right locations in the channel. After that, the two parts were kept in contact for 1 hour. Finally, the whole system was assembled.

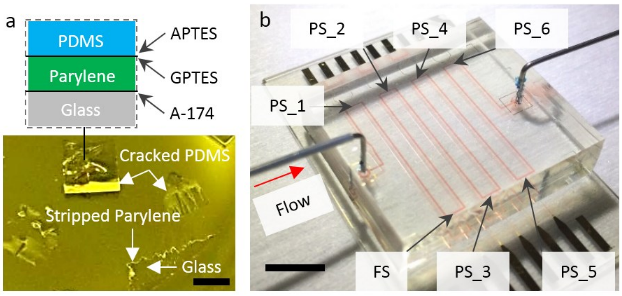

Figure 3: Image of the real device (a) Delamination test results. Scale bars, 5mm. (b) Fully developed device with six PSs and one FS in the channel for local pressure monitoring.

The bonding strength of Parylene-glass and Parylene-PDMS was tested through delamination tests (Fig. 3a). Both the assembly of Parylene-glass and Parylene-PDMS exhibits robust bonding strength. The fully developed system is shown in Fig. 3b, a winding channel with seven turnings is highlighted by blue solution. Six bubble PSs and a FS are located within the channel and along the flow.

RESULTS AND DISCUSSION

Bubble generation

The SEM image of the micro chamber is shown in Fig. 4a. The micro chamber is closed at one end and open at the other end. When some liquid is applied to it, the liquid can wick into the micro chamber. Since the sharp corners of the interior of the micro chamber are prone to wet, the inner gas will be trapped by the wetting phase in the corners, then forming a bubble in the chamber. Note that the slightly hydrophobic surface of Parylene-C is treated with oxygen plasma to render the inner surface of the micro chamber hydrophilicity. The slow motion of the generation process in the micro chamber appears in Fig. 4 c-g.

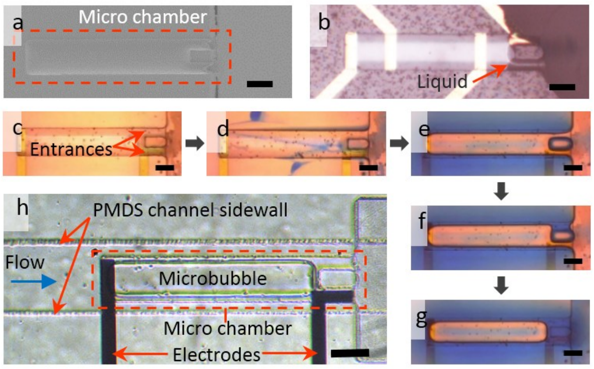

Fig. 4: Bubble generation based on spontaneous imbibition. (a) SEM image of the bubble PS. (b) Failure to generate a bubble before the surface modification. (c- g) Slow-motion of a bubble generation process out of the PDMS channel. (f) A bubble generated in the micro chamber within the PDMS channel. Scale bars, 100 µm.

Responds of the bubble PS.

Electrochemical impedance of the bubble PS was obtained via a precision LCR meter (WK 41100). Static pressure responses of the bubble PS were measured (1 kHz, 50 mv) in 1X PBS. Highly linear response and a calibrated sensor response of -274.6 Ω/ mmHg for 1X PBS were obtained by a linear fitting process (Fig. 5).

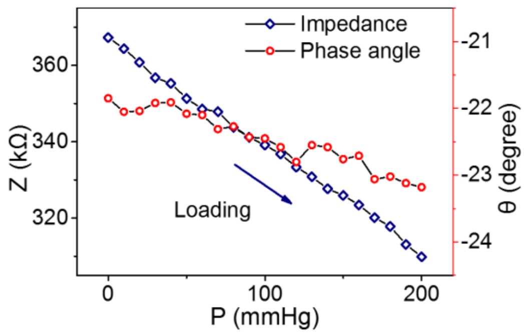

Figure 5: Response of the bubble PS to static pressure.

The bubble PS is also able to detect dynamic pressures, as shown in Fig. 6. The pressure of the solution, in which the sensor is immersed, was altered by pushing and releasing an airbag. A random pressure wave (1 Hz) was generated and recorded through a commercial PS (Honeywell 40PC), and compared with the outputs of the bubble PS. Results indicate that the two waves are almost the same.

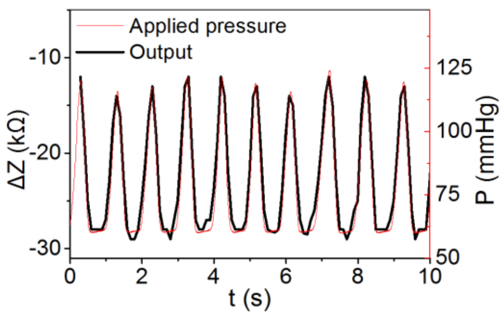

Figure 6: Responds of the bubble PS to dynamic pressure, compared with a commercial PS.

Local pressure monitoring

For device characterization, the inlet was attached to a constant pressure source and the outlet was open, thus a laminar flow was generated in the channel. Before the solution was applied, the whole device was treated with oxygen plasma. Bubbles were generated inside the micro chambers when the liquid flowed over the sensors (Fig. 4h). The impedance of each bubble PS was recorded through a LabVIEW program. For calibration, initial impedance, Z_0, of each sensor was recorded in absence of applied pressure (Fig. 7).

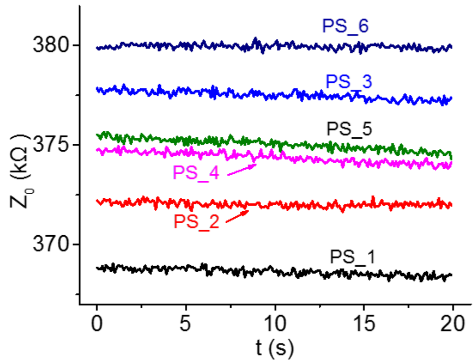

Fig. 7: Impedance recording of the six PSs without applied pressure.

Then, a stable pressure (120 mm Hg) was applied. Final results are shown in Fig. 8. As expected for laminar flows, we can observe a linear pressure drop along the flow direction.

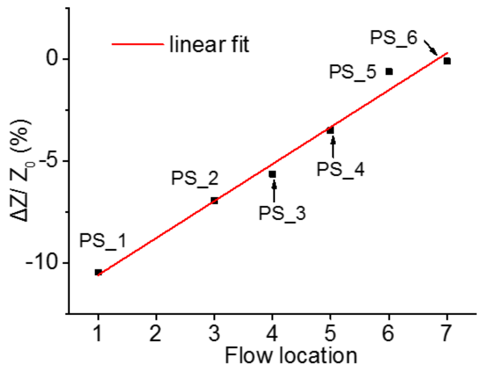

Figure 8: Normalized impedance changes of the six bubble PSs with the applied pressure of 120mmHg at the inlet.

Flow monitoring

We additionally show a versatile flow sensor (FS). The prototype of the FS shown in Fig. 9 has the same layout of electrodes as the bubble PS. The impedance measured with different frequencies of excitation alternating current (AC) can reflect different flow parameters. For example, the impedance measured at lower AC frequencies (< 500 Hz) can reflect the flow rate, as the capacitance of the electrical double layer (EDL) is sensitive to flow rate (Fig. 9a) [13-14]. While at higher frequencies (>1 kHz) the impedance can reflect the "things" in the fluid that change the resistance of the solution. For demonstration, we injected a bubble into the channel and recorded the impedance change when it flowed over the FS. We observed more than two orders of magnitude changes in the impedance (Fig. 9 b-d).

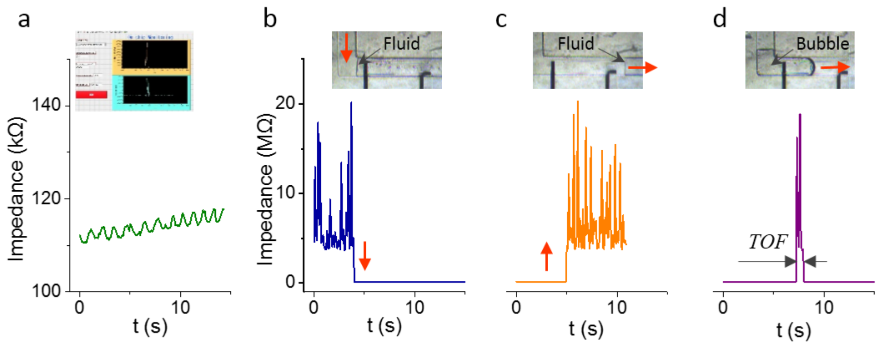

Fig. 9: Multifunctional flow monitoring. (a) In-channel flow rate monitoring with a LabVIEW interface. (b) Flow beginning recording. (c) Flow ending recording. (d) Bubble monitoring.

CONCLUSION

We proposed a new design of microfluidic system. It consists of two subsystems, a conventional PDMS channel subsystem, and the sensing subsystem with electrical readouts. The sensing subsystem is integrated with multiple sensors that can simultaneously monitor multiple parameters in the channel. The prototype and as-fabricated device have demonstrated the ability of real-time monitoring local pressure and flow condition within the channel. Microfluidic system integrated with multiple sensors within the channel is the first time realized. In future studies, more sensors that are process-compatible with the smart substrate, such as temperature sensor, will be added to the sensing subsystem to realize higher integration and more intelligent microfluidic systems. This design may open the application of feed-back and accurate control for microfluidic systems.

ACKNOWLEDGEMENTS

The authors would like to thank the Center for Advanced Electronics Materials and Devices (AEMD), Shanghai Jiao Tong University, for micromachining technique supports.

REFERENCES

[1] A. Riaud, et al. “A facile pressure drop measurement system and its applications to gas–liquid microflows”, *Microfluidics and Nanofluidics,* vol. 15, no.5, pp. 715-724, 2013.
[2] A. Lai, M. Fuerstman, M. Thurlow, et al. “The pressure drop along rectangular microchannels containing bubbles”, *Lab on A Chip,* vol. 7, no. 11, pp. 1479-1489 2007.
[3] C. Y. Wu, et al., “Integrated electrofluidic circuits: pressure sensing with analog and digital operation functionalities for microfluidics”, *Lab on A Chip,* vol. 12, no. 20, pp. 3943-3951, 2012.
[4] C. Y. Wu, W. H. Liao, and Y. C. Tung. “Integrated ionic liquid-based electrofluidic circuits for pressure sensing within polydimethylsiloxane microfluidic systems”, *Lab on A Chip*, vol. 11, no. 10, pp. 1740-1746, 2011.
[5] K. Chung, H. Lee, and H. Lu, “Multiplex pressure measurement in microsystems using volume displacement of particle suspensions”, *Lab on A Chip*, vol. 9, no. 23, pp. 3345-3353, 2009.
[6] A. Orth, E. Schonbrun, and K. B. Crozier, “Multiplexed pressure sensing with elastomer membranes”, *Lab on A Chip,* vol. 11. no. 11, pp. 3810-3815 (2011).
[7] T. Jung, and S. Yang, “Highly Stable Liquid Metal-Based Pressure Sensor Integrated with a Microfluidic Channel”, *Sensors,* vol. 15, no. 5, pp. 11823-11835, 2015.
[8] O. Ozsun, et al., “Non-invasive measurement of the pressure distribution in a deformable micro-channel”, *Journal of Fluid Mechanics*, vo. 734, no. 8, pp. 1222-1238, 2013.
[9] M. J. Kohl, et al. “A microfluidic experimental platform with internal pressure measurements”, *Sensors & Actuators A Physical,* vol. 118, no. 2, pp. 212-221, 2005.
[10] N. Srivastava, and M. A. Burns, “Microfluidic pressure sensing using trapped air compression”, *Lab on A Chip*, vol. 7, no. 5, pp. 633-637, 2007.
[11] U. Gowrishetty, et al. “Development of ultra-miniature pressure sensors for 1-French biomedical applications and beyond”, *Sensor Lett.*, vol. 6, pp. 433-440, 2008.
[12] P. Starr, K. Bartelsc, M. Agrawalb, and S. Bailey, “Evolution of micromachined pressure transducers for cardiovascular applications”, *Sens. Actuators A Phys.,* vol. 225, pp. 8-19, 2015.
[13] Jongin Hong, et al., “AC frequency characteristics of coplanar impedance sensors as design parameters,” *Lab Chip*, vol. 5, p. 270-279, 2005.
[14] Nima Arjmandi, Chengxun Liu, Willem Van Roy, Liesbet Lagae, Gustaaf Borghs, “Method for flow measurement in microfluidic channels based on electrical impedance spectroscopy,” *Microfluidics and Nanofluidics*, vol. 12, no. 1, p. 17-23, 2012.
[15] L. Tang, J. Liu, and B. Yang. “An ultraflexible microbubble blood pressure sensor for interventional treatment”, *IEEE International Electron Devices Meeting IEEE*, pp. 767-770, 2015.
[16] L. Tang, and N. Y. Lee. “A facile route for irreversible bonding of plastic-PDMS hybrid microdevices at room temperature”, *Lab on A Chip,* vol. 10, no. 10, pp. 1274-80, 2010.

CONTACT

*J.Q. Liu, Tel: +86-21-34207209; jqliu@sjtu.edu.cn